J. Nanoanalysis., 7(2): 104-114, Spring 2020

RESEARCH ARTICLE

An efficient platform based on cupper complex-multiwalled carbon nanotube nanocomposite *modified electrode* for the determination of uric acid

Mohammad Mehdi Foroughi

Department of Chemistry, Kerman Branch, Islamic Azad University, Kerman, Iran

ARTICLE INFO

Article History:
Received 2019-08-05
Accepted 2020-01-13
Published 2020-05-01

Keywords:
Uric acid
Cupper complex
Multiwalled carbon nanotube
Modified electrode

ABSTRACT

A new voltammetric sensor for determination of uric acid (UA) by Cupper complex- multiwalled carbon nanotube (Cu-$_{complex}$-CNT) nanocomposite modified carbon paste electrode (CPE) is reported. The electrocatalytic behavior of the Cu-$_{complex}$-CNT nanocomposite modified CPE was studied in pH 2.0 phosphate buffer solution by chronoamperometry (CA) and cyclic voltammetry (CV) in the presence of uric acid. Due to the excellent electrocatalytic activity, enhanced electrical conductivity and high surface area of the Cu-$_{complex}$-CNT, determination of uric acid with well-defined peaks was achieved at the Cu-$_{complex}$-CNT modified electrode. The catalytic peak current obtained, was linearly dependent on the UA concentrations in the range of 0.66 – 350.0µM with sensitivity of 0.05 µA µM-1. The detection limits for UA were 0.075µM, The diffusion coefficient for the oxidation of UA at the modified electrode was calculated as (4.1±0.05) ×10−5 cm2 s−1. The proposed sensor was successfully examined in real sample analysis with urine and human serum and revealed stable and reliable recovery data.

How to cite this article
Foroughi M.M. An efficient platform based on cupper complex-multiwalled carbon nanotube nanocomposite modified electrode for the determination of uric acid. J. Nanoanalysis., 2020; 7(2): 104-114. DOI: 10.22034/JNA.2020.1875990.1152.

INTRODUCTION

Uric acid (2,6,8-trihydroxypurine, UA), is main final products of the cellular metabolic breakdown of purine nucleotides, adenosine and guanosine in the human body [1]. Uric acid is an important analyze in clinical field and plays a significant role in bioelectrochemistry and clinical diagnostics applications. Normal UA serum levels range from 41 to 88mgmL^{-1} and urinary excretion is usually 250–750mg per day [2]. It has been shown that abnormal concentration levels of UA in the human body could be caused by such diseases like Lesch–Nyan syndrome, chronic renal, gout, cardiovascular and kidney damage [3,4]. Hence, monitoring the concentration of UA in biological fluids may be used as an early warning of the presence of kidney diseases. There are many methods for the determination of UA, such as enzymic colorimetric [5], chemical [6], chemiluminescence [7], fluorescence [8], voltammetric–colorimetric [9], high-performance liquid chromatography (HPLC) [10,11], and enzymatic–spectrophotometric [12]. These methods suffer from some disadvantages, such as the complex operating process, expensive instruments and strict pre-disposal. In recent years electrochemical procedures because of their simplicity, less time consuming, ease of miniaturization, high sensitivity and relatively low cost as compared to other technique have been extensively investigated for the determination of UA. In general, the electrochemical methods for monitoring UA could be classified as non-enzymatic and enzymatic methods.

Enzymatic methods include irreversibly oxidization of uric acid with uricase [13,14] to produce allantois and H_2O_2 [15] and then the determination of H_2O_2. But this technique is expensive and difficult. In order to overcome these difficulties, many efforts have been carried out for developing novel materials used for modifying the electrode and various modified electrodes using nanoparticles [16,17], polymer film [18], metal oxide nanopar-

* Corresponding Author Email: *foroughi@iauk.ac.ir*

ticles [19], ionic liquid [20] and carbon nano materials [21] have been constructed. In recent years, much attention has been given to the development of novel nanostructures, which are used for signal amplification in electrochemical sensors [22-29]. Nanomaterials are usually used to take advantage of a larger surface area for biomolecules to be immobilized [30-39]. Carbon nanotubes (CNTs) have received enormous attention in the recent years due to their unique structural, mechanical, geometric and chemical properties. Because of high surface area and electronic properties of carbon nanotubes they used in construction of electrochemical sensors [40,41] as a promote electron transfer. Also, the copper can be used for many applications including buffer layer and contact for device fabrication, photocatalytic etc [42].

In this paper, we proposed for the first time the application of a modified CPE using MWCNTs and CU complex for determination of UA. Low detection limits and high sensitivity for UA was obtained due to the high electrocatalytic properties of MWCNTs and Cu complex. We evaluated Analytical performance of this sensor for determination of UA by voltammetry. Finally, this sensor has been used for the determination of UA in urine and human serum as real sample.

EXPERIMENTAL

Reagents and solutions

The UA was purchased from Sigma-Aldrich and used as received. The stock solution of UA solution (0.01 M) was prepared by dissolving appropriate amount of UA in a small volume of .1 mol L^{-1} NaOH olution and diluted to reach desired concentration. The solution was kept in a refrigerator in the dark. More dilute solutions were prepared by serial dilution phosphate buffer solutions. Multiwall carbon nanotubes (MWCNT), with nanotube diameters, OD = 20–30 nm, wall thickness = 1–2 nm, length = 0.5–2 m and purity of >95% was purchased from Aldrich. A series of buffer solution including H_3PO_4 were prepared and pHs were adjusted using NaOH (0.1 M) in the range from 1.0 to 6.0. The other reagents used were analytical reagent grade and all solutions were prepared with double distilled deionized water. All the chemicals were used without further purification.

Apparatus

IR spectrum was recorded on a FT-IR JASCO 680-PLUS spectrometer (20 spectra/sec, 16 cm^{-1} resolution, MCT-W detector) using KBr pellets from 4000-400 cm^{-1}. The surface morphology of the composites was analyzed with KYKY, EM 3200 Scanning Electron Microscopy (SEM). Electrochemical measurements were performed with an SAMA500 Electroanalyser (SAMA Research Center, Iran) controlled by a personal computer. The three-electrode cell system consisted of carbon past working electrode (modified or unmodified), a saturated calomel electrode (SCE) as reference electrode and a Pt wire electrode as the auxiliary electrode. All the electrochemical experiments were carried out under a pure nitrogen atmosphere at room temperature.

Synthesis of [Cu(Cip)(phen)](NO_3).4H_2O

A solution of 1,10-phenantroline (49.6 mg, 0.25 mmol) was added to a suspension of sodium ciprofloxacinate (102.5 mg, 0.25 mmol). After 10 min of vigorous stirring, a solution of $Cu(NO_3)_2.3H_2O$ (60.5 mg, 0.25 mmol) was added. The solvent used to be a mixture of MeOH: H_2O (1:1) and the final volume was 50 mL. The pH was adjusted to 7.84 with 1 M NaOH. The solution was irradiated by sonochemical with the power of 60 W and temperature 50 °C for 30 min. The obtained precipitates were filtered, subsequently washed with water and then dried. The elemental analysis and IR spectra of the nano-structure produced by the sonochemical method as well as the bulk material produced by literature [43]. Anal. Calc. for $C_{29}H_{33}N_6O_{10}FCu$: C, 49.15%; H, 4.66%; N, 11.86%. Found: C, 48.67%, H, 4.73%; N, 11.79%, Cu, 8.81%. IR (KBr): ν(O–H and N–H) = 3600-2300 cm^{-1}; ν(C=O) = 1730 cm^{-1}; ν(C=N) = 1610 cm^{-1}; ν(arC–C) = 1514 cm^{-1}.

Fig. 1 shows a representative SEM image of [Cu(Cip)(phen)](NO_3).4H_2O nanoparticles. Sphere-like [Cu(Cip)(phen)](NO_3).4H_2O nanoparticles with a size of ~50 nm were directly synthesized by ultrasonic method. The SEM image shows that there are some small holes inside the product, which indicate that it can be used in catalysis.

Preparation of the modified electrode

Modified electrode was made by hand mixing of CU complex, graphite powder and MWCNT (1.0, 89 and 10 percent respectively) with a mortar and pestle. Paraffin (Dc 350, Merck) was added to the above mixture using a 5mL syringe and mixed for 20min until a uniformly wetted paste was obtained. The paste was then packed into the end of a glass tube (ca. 2mm i.d. and 10 cm long). Electrical con-

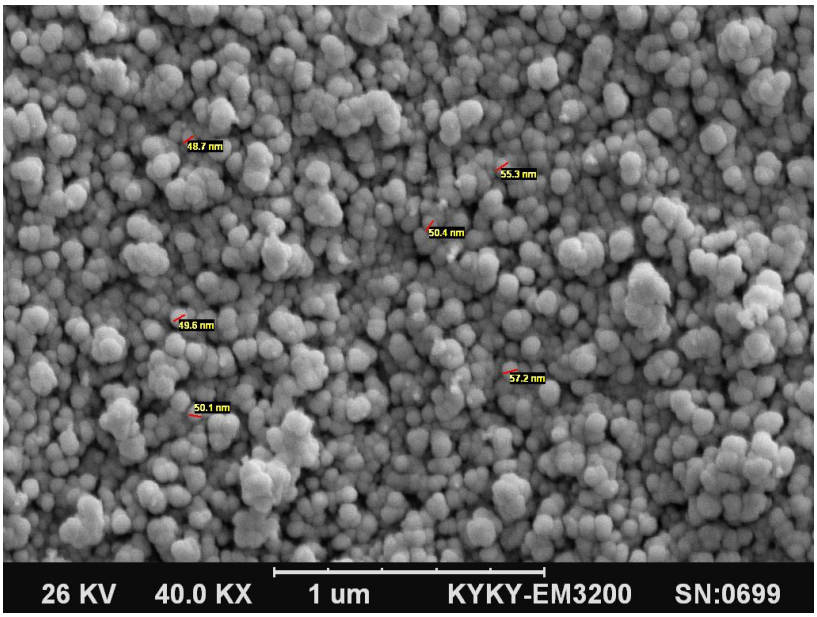

Fig. 1. SEM image of [Cu(Cip)(phen)](NO_3).4H_2O nanoparticles.

tact was made by inserting a copper wire into the glass tube at the back of the mixture. When a new surface was necessary, it was obtained by pushing an excess of paste out of the tube and polishing it on a weighing paper. The efficiency of the modified electrode for the determination of real samples was maintained for more than one week. Unmodified carbon paste was made in the same way without adding Cu complex and carbon nanotube to the mixture and was used for comparison purposes.

RESULTS AND DISCUSSION

Electrochemical properties of $Cu_{\text{-complex}}$ - CNTPE

Cyclic voltammograms of $Cu_{\text{-complex}}$ - CNTPE in PBS (pH 2) at different scan rates are shown in Fig. 2. A pair of reduction and oxidation peak at 0.178 and 0 .201 was appeared and 0.23m V potential peak separation was obtained. The corresponding plot for the anodic peak current (Ipa) and catodic peak current (Ipc) as a function of scan rate (υ) is shown as inset in Fig. 2B was linearly dependent on the scan rate (υ) over the range of 5–450mVs^{-1}, with the regression equation Ipa (μA) = 0.0164υ + 0.9765 (correlation coefficient, r = 0.9933) and Ipc (μA) = –0.165υ – 0.9229 (correlation coefficient, r = 0.9972), indicating a surface-controlled electrode processes. From the behavior of the modified $Cu_{\text{-complex}}$ - CNTPE with scan rate, we can conclude that the electrode reaction was a diffusion less system and a reversible electron transfer. The peaks can be attributed to redox reaction of Cu (II) to Cu (I), assumed to be a reversible one-electron transfer:

$$Cu(II) + e \underset{\rightarrow}{\leftarrow} Cu(I) \quad (1)$$

The influence of scan rate on the redox peak potential was also studied. Based on the results with the increase of scan rate, potential of the oxidation peak shifted positively and potential of the reduction peak shifted negatively. Laviron and coworker [44] demonstrated that the kinetic electrochemical parameters (ks and) could be derived:

$$E_{pc} = E^{0'} - 2.3RT\frac{\log\upsilon}{\alpha nF} \quad (2)$$

$$E_{pa} = E^{0'} + 2.3RT\frac{\log\upsilon}{(1-\alpha)nF} \quad (3)$$

Where α is the electron transfer coefficient, n is the electron transfer number, v is the scan rate, other symbols have their normal meanings. AS can be seen in Fig.2D, the E_{pa} and E_{pc} were linearly dependent on the logv with the regression equations of E_{pa} = 0.0563logv + 0.1037 (V, mVs^{-1}, R = 0.9973) and E_{pc} =–0.0363logv – 0. 243 (V, mVs^{-1}, R = 0.9918). Base on slope of this equations and number of electron involved n=1, α was calculated to be 0.607.

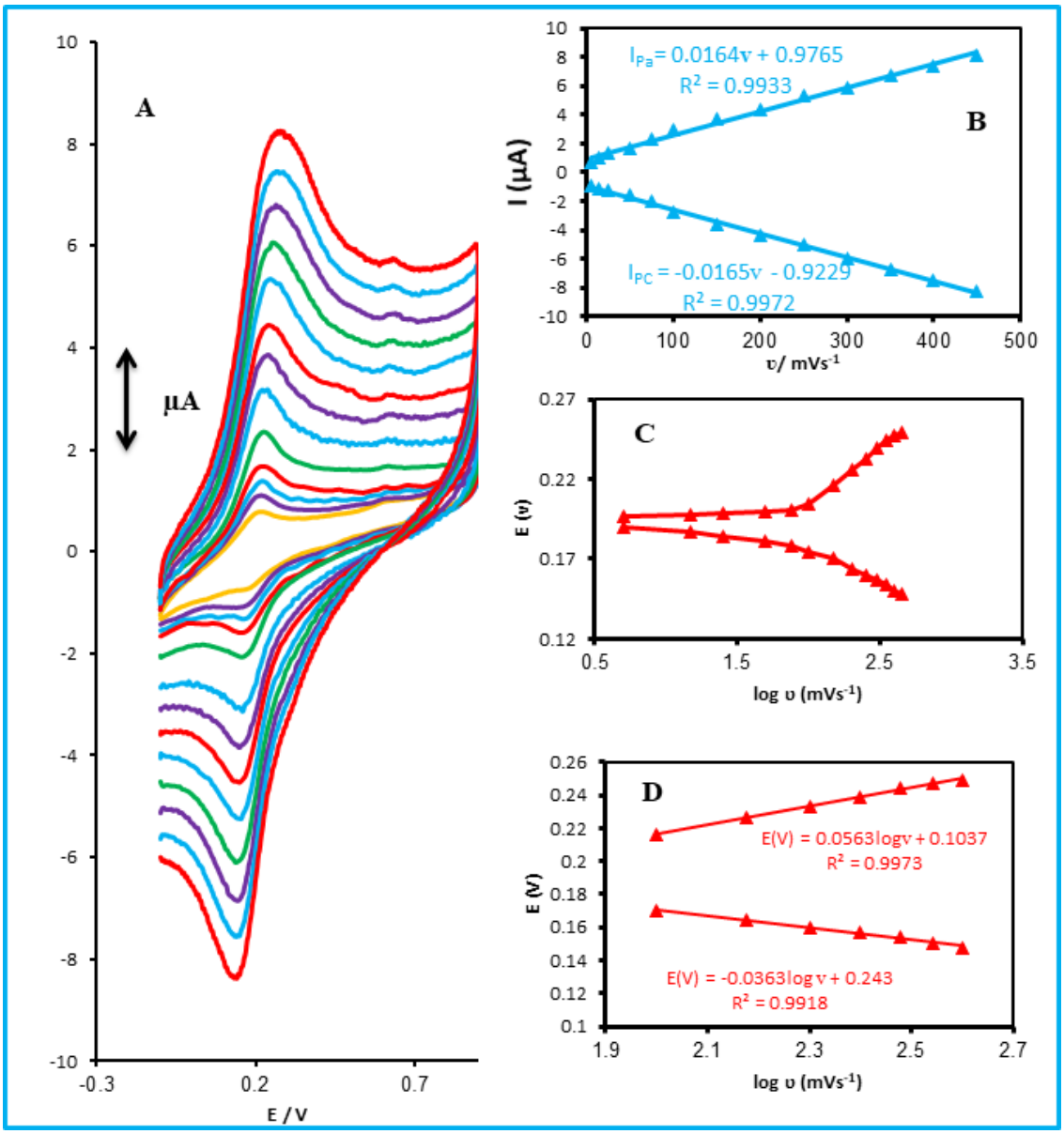

Fig. 2. (a) CVs of $Cu_{\text{-complex}}$-CNTPE electrode in pH (2) at various scan rates (from inner to outer curve): 5, 15, 25, 50, 75, 100, 150, 200, 250, 300, 350, 400 and 450 mV s^{-1}. (b) The plot of peak currents vs. scan rates.

Voltammetric behaviors of UA

Electrochemical behaviors of the UA (200 μM) in 0.1M PBS of pH 2 was carefully investigated at the surfaces of bare CPE, $Cu_{\text{-complex}}$- CPE and $Cu_{\text{-complex}}$-CNTPE using cyclic voltammetriy. CPE electrodes showed a weak and a broad oxidation peak for a UA at 0.608V (see Fig. 3) suggesting slow electron transfer kinetics. In contrast, when $Cu_{\text{-complex}}$ -CPE was applied well defined sharp peak appeared. As is shown, the oxidation peak for UA at the $Cu_{\text{-complex}}$ -CPE is several times larger than unmodified electrode. This increase is due to the catalytic effect of Cu complex. At last, when carbon nanotubes added to electrode composite, the peak showed an increase because of large specific surface area and high electrical conductivity of carbon nanotubes. It was also noted that the reduction current responses to the oxidation product of UA on the three type electrodes were all negligible, which indicated that the electrochemical redox of UA at these electrodes was irreversible.

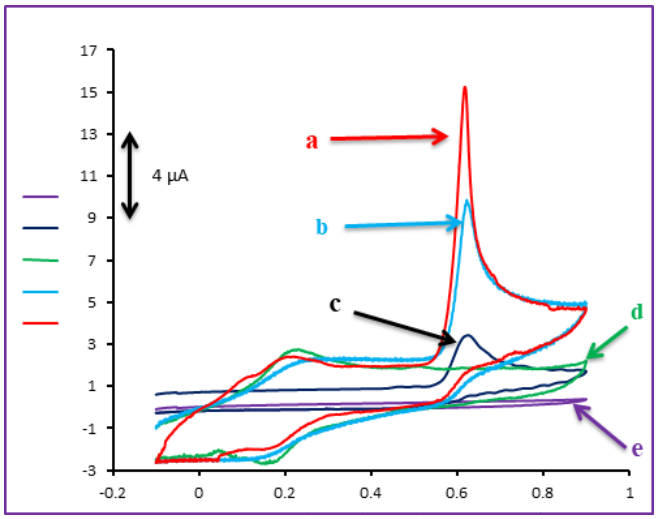

Fig. 3. (a) CV at BCPE, (b) $Cu_{\text{-complex}}$-CPE (c) $Cu_{\text{-complex}}$-CNTPE electrodes in the presence of UA (250.0 µM), (d) and (e) as (c) and (a) in absence of UA in PBS (0.1 M) at pH 2.0. Scan rate: 50 mV s^{-1}.

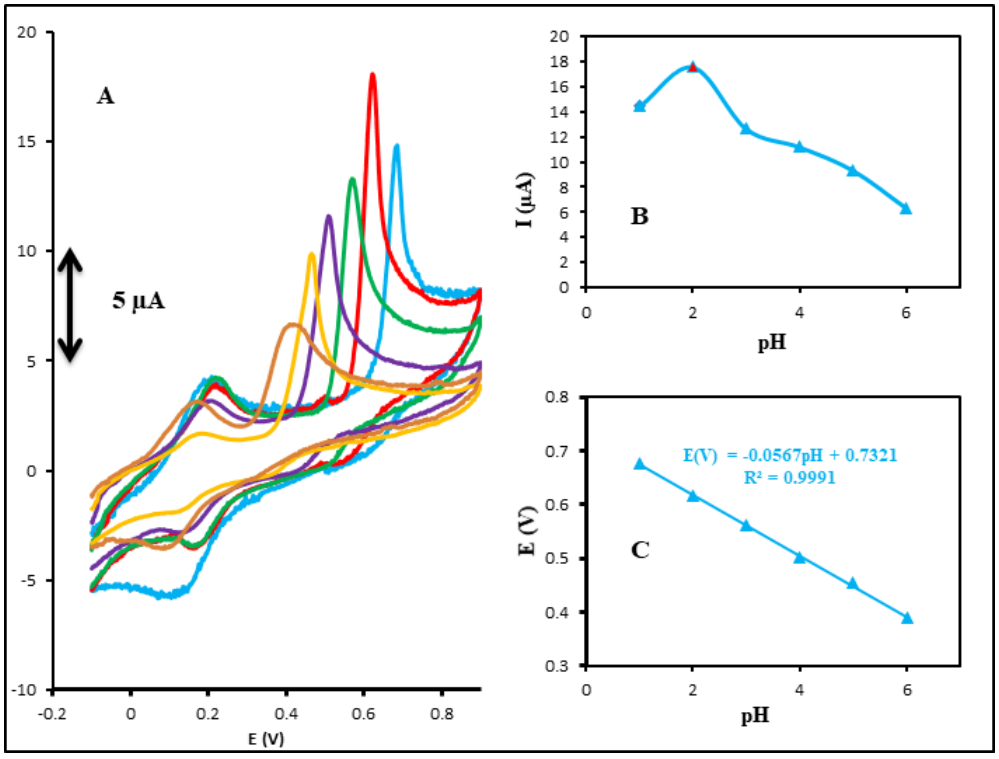

Fig. 4. (a) Effect of pH on the peak separation and peak current for the oxidation of UA (250 µM); pH= 1.0 – 6.0. Scan rate, 50 mVs^{-1}. (b) Plot of peak currents vs. pH. (c) Plot of peak potential vs. pH.

Effect pH on the oxidation of UA

The acidity of electrolyte has a significant influence on the UA electrooxidation because protons take part in the electrode reaction. The effect of pH on $Cu_{\text{-complex}}$ - CNTPE signal were carefully investigated by cyclic voltammetry using 0.1 mol L^{-1} buffer solutions at pH levels ranging from 1 to 6. The results were shown in Fig. 4A. Based on the

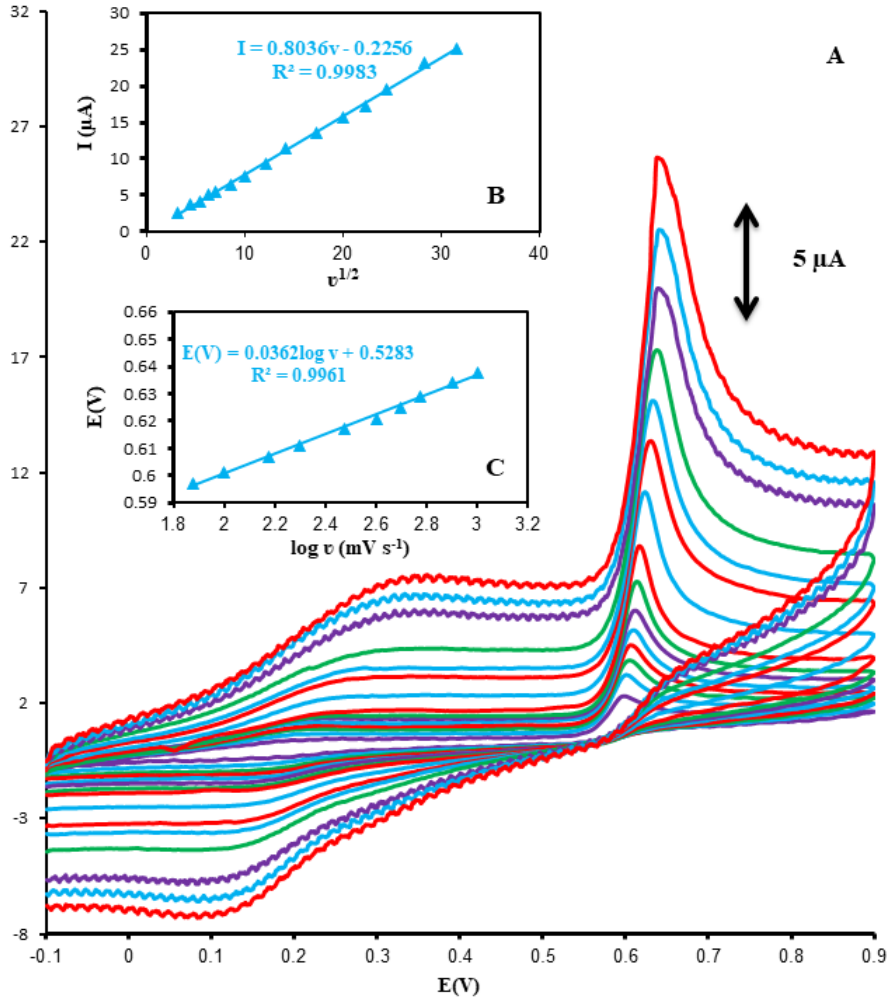

Fig. 5. (a) CVs of UA (50µM) at $Cu_{-complex}$-CNTPE electrode in pH (2) at various scan rates (from inner to outer curve): 10, 20, 30, 40, 50, 75, 100, 150, 200, 300, 400, 500, 600,800 and 1000 mV s^{-1}. (b) The plot of peak currents vs. scan rates, (C)plot of peak potential vs. scan rates.

results, the peak current UA increases slightly with an increase in the solution pH until it reaches 2 and then decrease. It can be seen from Fig. 4B that the highest peak current was obtained at pH 2. It was observed that as pH of the medium was gradually increased, peak potentials for the oxidation of UA shifted towards less positive values, showing that protons have taken part in their electrode processes. Out of these, phosphate buffer solution with pH 2 gave the best response in terms of peak current and peak shape and negatively shifts, hence was chosen as optimal pH for further studies. Plot of Ep vs. pH for UA in the working pH range was shown in Fig. 4C. As can be seen, the Ep of UA has linear relationship with pH of the buffer solution regarding following equations:

UA: Ep (V) = 0.0567 – 0.7321pH
(R2 = 0.9991) (5)

Regarding the observed slopes of 0.0567 mV/pH for UA which was close to the anticipated Nernstian value for a two-electron, two-proton electrochemical reaction [28]. It can be concluded that equal number of electrons and protons are involved in the electrode reactions.

Influence of scan rate on the electrochemical behavior of UA

The influence of scan rate on the oxidation peak current of UA was investigated on $Cu_{-complex}$ - CNTPE by cyclic voltammetry. As can be seen in Fig. 5 A, the peak current intensity increases continuously with the increase of scan rate. Fur-

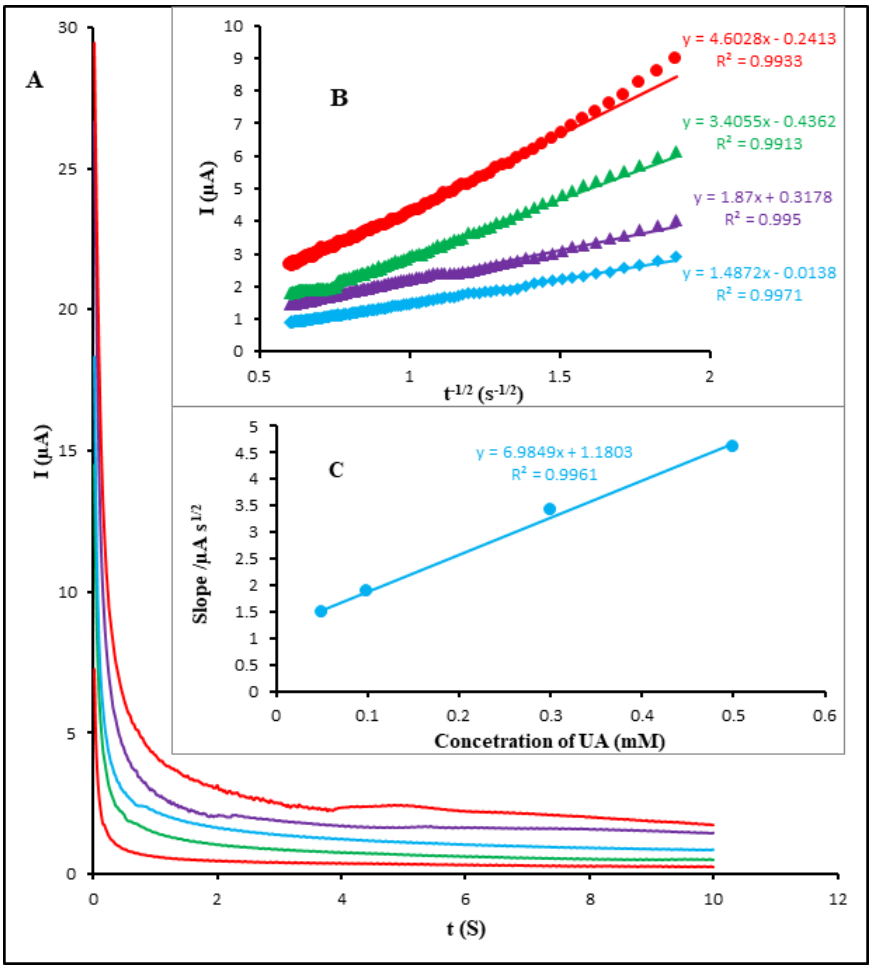

Fig. 6. (a) Chronoamperograms obtained at $Cu_{-complex}$-CNTPE in 0.1 M PBS (pH 2.0) for different concentration of UA. The numbers 1–5 correspond to:s 0.0, 0.05, 0.1, 0.3 and 0.5 mM of EP. Insets: (c) Plots of I vs. $t^{-1/2}$ obtained from chronoamperograms 1–5. (b) Plot of the slope of the straight lines against UA concentration.

thermore, the current was directly proportional to the square root of the scan rate over the range of 10–1000 mV s^{-1} as shown in Fig. 5B, which powerfully proposed that the redox reactions of UA are diffusion controlled. The influence of scan rate on the redox peak potential was also studied. Based on the results with the increase of scan rate, the potential of the oxidation peak shifted positively .Laviron and coworker demonstrated that the kinetic electrochemical parameter (α) could be derived.

The relationship between the anodic peak potential (Epa) and logarithm of the scan rate (log) for UA was also constructed and followed the linear regression equation of Epa (V) = 0.0589logv (mVs^{-1}) + 0.47 (R = 0.9902) in the range from 75 to 1000 mVs^{-1}. For a completely irreversible electrode process, the relationship between Epa and logv is expressed as follows by Laviron:

$$E_{pa} = E^0 + \left(\frac{RT}{\alpha nf}\right)\ln\left(\frac{RTK^{\circ}}{\alpha nf}\right) + 2.3RT\frac{\log\upsilon}{\alpha nF} \quad (6)$$

Because the electron number involved in the oxidation process is 2, α was calculated to be 0.498.

Chronoamperometric study

Chronoamperometric measurements of UA at $Cu_{-complex}$ - CNTPE were also studied by setting the working electrode potential at 0.65 V vs. SCE for the various concentration of UA in PBS (pH 2) (Chronoamperogram for UA was shown in Fig. 6). For an electroactive with a diffusion coefficient

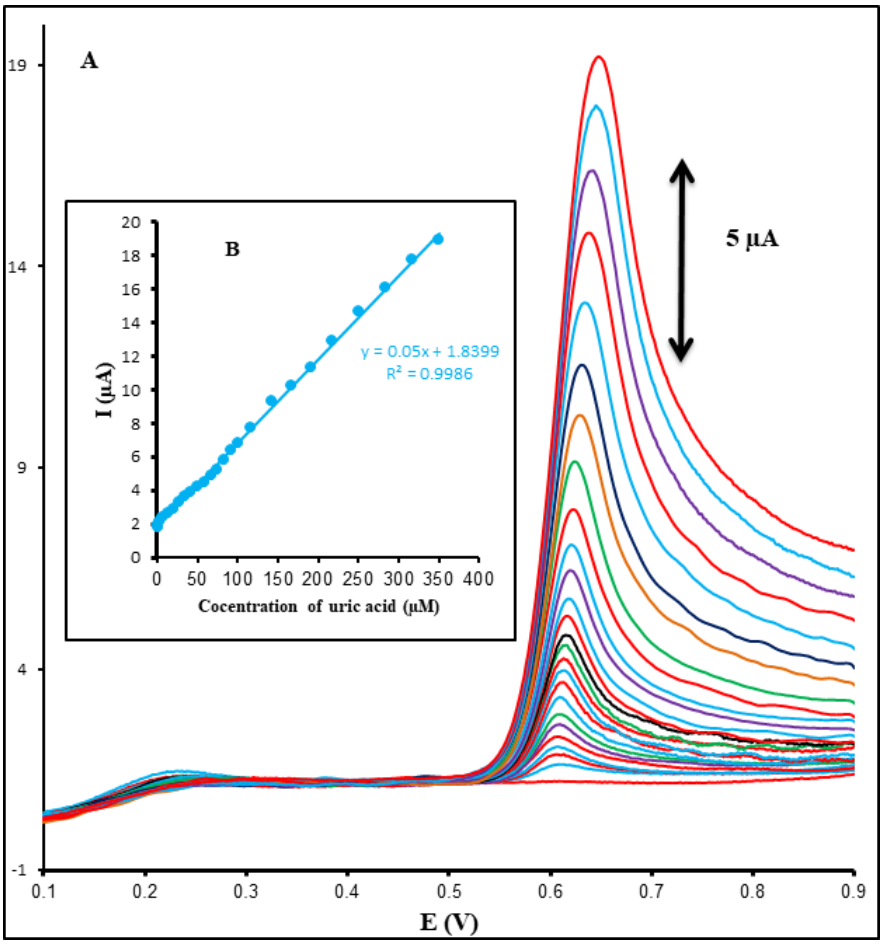

Fig. 7. (A) CV of UA at the $Cu_{\text{-complex}}$ - CNTPE electrode in phosphate buffer solution (pH 2.0) at the scan rate of 50 mV s^{-1}. Concentrations from inner to outer of curves: UA (0.0, 0.66, 1.66, 3.33,6.66, 13.3, 20.0, 26.6, 33.3, 461.6, 50.0, 58.3, 66.6, 75.0 ,83.3, 91.6, 100.0, 116.6, 141.6, 166.6, 191.6, 216.6, 250, 283.3, 316.6 and 350). Insets: (B) Plots of I vs. Concentrations.

of D, the current for the electrochemical reaction with a mass transport limited rate is described by the Cottrell equation [45].

$$I = nFAD^{1/2}C_b\pi^{-1/2}t^{-1/2} \quad (8)$$

For example, under diffusion control, a plot of I vs. $t^{-1/2}$ will be linear, and the slope of the linear region of the Cottrell's plot can be used to estimate of the D for UA. The value of D_{UA} was found to be 4.1×10^{-5} cm^2 s^{-1}.

Determination of UA

The calibration curve for the UA electrochemical determination at the $Cu_{\text{-complex}}$ - CNTPE was characterized under the optimal experimental conditions using LSV technique (Fig. 7). Clearly the anodic peak current increases linearly with UA concentration ranging from 0.66 µM to 350.0 µM with a correlation coefficient of 0.9986. The liner regression equations for UA was Ip = 1.8399 + 0.05 C (µM) with a detection limit of 0.075 µM. The reproducibility and stability of the $Cu_{\text{-complex}}$ - CNTPE was also tested. The relative standard deviation (RSD) of 2.9% for 10 times parallel detections of 100.0 µM UA solution, proved a good reproducibility of proposed electrode. After one month storage at room temperature, the current response of UA (100.0 µM) had 93% of the initial response current remained showing that the $Cu_{\text{-complex}}$ - CNTPE had noble stability. The good reproducibility and stability proved that the electrode was suitable for analysis of practical samples.

Table 1. Determination of UA in human serum and urine samples using $Cu_{-complex}$-CNTPE (n = 5).

Sample	Analyte	Detected (μM)[a]	Added (μM)	Found (μM)[a]	Recovery (%)
Serum	UA	ND[b]	30.0	28.9±1.8	96.4
			50.0	47.7±4.6	95.4
Urine	UA	1.85	30.0	30.9±4.3	97.1
			50.0	52.0±0.28	100.28

[a] Mean±standard deviation for n = 5.
[b] Not detect

Table 2. Comparison the proposed method with other electroanalytical methods with $Cu_{-complex}$-CNTPE electrodes for determination of UA.

Electrode	Modifier	Linear range (μM)	Detection limit (μM)	Ref.
Au electrode	Uricase onto AuNP/c–MWCNT	10 – 800	0.1	[46]
Glassy carbon	Poly(diallyldimethylammonium chloride	1.0 – 60	1.0	[47]
Glassy carbon	RTIL–NiHCF–NP-gel modified PIGE[a]	1.0 – 260	0.33	[48]
Glassy carbon	MWCNT–HoFNPs[b]	0.2 – 500	0.06	[49]
Carbon paste	Cu-complex- CNT	0.6 – 350.0	0.075	This work

[a] Room temperature ionic liquid/nickel hexacyanoferarrate nanoparticles composite paraffin wax impregnated graphite electrode graphite electrode.
[b] Holmium fluoride nanoparticles/multi-walled carbon nanotube

Real Sample analysis

In order to evaluate the analytical applicability of the developed method for determination of UA, urine and blood were tested. The amounts of UA in urine and blood sample were determined by the standard addition method and are listed in Table 1. The recoveries were 95.4–100.28% for UA, respectively. Therefore, a capability of the proposed electrode for the determination of UA is clear.

CONCLUSIONS

We have demonstrated a very simple and effective electrochemical approach to construct of a $Cu_{-complex}$- CNTPE sensor and its application for determination of UA. Compared with the unmodified CPE, the significant increase of peak current was observed at the $Cu_{-complex}$ - CNTPE, which clearly demonstrated that Cu complex and CNT could be used as an efficient promoter to enhance the kinetics of the electrochemical process of UA. The optimization of the experimental conditions for LSV yielded a detection limit for UA of 0.075 μM better than or comparable those described in the literature (Table 2). In addition, the proposed sensor was successfully applied for determination of UA in urine and blood samples with satisfactory results.

CONFLICT OF INTEREST

The authors declare that there is no conflict of interests regarding the publication of this manuscript.

REFERENCES

1. W. Arneson, and J. Brickell, Clinical Chemistry: A Laboratory Perspective, F.A. Davis Company, Philadelphia, USA (2007).
2. Alderman M. Uric acid and cardiovascular risk. Current Opinion in Pharmacology. 2002;2(2):126-30.
3. Kannan P, John SA. Determination of nanomolar uric and ascorbic acids using enlarged gold nanoparticles modified electrode. Analytical Biochemistry. 2009;386(1):65-72.
4. Arslan F. An Amperometric Biosensor for Uric Acid Determination Prepared From Uricase Immobilized in Polyaniline-Polypyrrole Film. Sensors. 2008;8(9):5492-500.
5. Lorentz K, Berndt W. Enzymic determination of uric acid by a colorimetric method. Analytical Biochemistry. 1967;18(1):58-63.
6. Isdale IC, Buchanan MJ, Rose BS. Serum Uric Acid Estimation: A Modified Chemical Method. Annals of the Rheumatic Diseases. 1966;25(2):184-5.
7. Yao D, Vlessidis AG, Evmiridis NP. Monitoring reactive oxygen species in vivo using microdialysis sampling and chemiluminescence detection as an alternative global method for determination of total antioxidant capacity. Analytica Chimica Acta. 2002;467(1-2):133-44.
8. J. Galban, Y. Andreu, M.J. Almenara, S. de Marcos, and J.R. Castillo, Direct determination of uric acid in serum by a fluorometric–enzymatic method based on uricase, Talanta, 54, 847 (2001).
9. I.F. Abdullin, Y.N. Bakanina, E.N. Turova, G.K. Budnikov, Determination of uric acid by voltammetry and coulometric titration, J. Anal. Chem., 56, 453 (2001).
10. Wang J, Golden T, Peng T. Poly(4-vinylpyridine)-coated glassy carbon flow detectors. Analytical Chemistry. 1987;59(5):740-4.
11. Greenberg ML, Hershfield MS. A radiochemical-high-performance liquid chromatographic assay for urate oxidase in human plasma. Analytical Biochemistry.

1989;176(2):290-3.
12. Bhargava AK, Lal H, Pundir CS. Discrete analysis of serum uric acid with immobilized uricase and peroxidase. Journal of Biochemical and Biophysical Methods. 1999;39(3):125-36.
13. Gao Z, Siow KS, Ng A, Zhang Y. Determination of ascorbic acid in a mixture of ascorbic acid and uric acid at a chemically modified electrode. Analytica Chimica Acta. 1997;343(1-2):49-57.
14. Zhang L, Lin X. Covalent modification of glassy carbon electrode with glutamic acid for simultaneous determination of uric acid and ascorbic acid. The Analyst. 2001;126(3):367-70.
15. Shi K, Shiu K-K. Determination of Uric Acid at Electrochemically Activated Glassy Carbon Electrode. Electroanalysis. 2001;13(16):1319-25.
16. Wang P, Li Y, Huang X, Wang L. Fabrication of layer-by-layer modified multilayer films containing choline and gold nanoparticles and its sensing application for electrochemical determination of dopamine and uric acid. Talanta. 2007;73(3):431-7.
17. M. Nazari, S. Kashanian, and R. Mohammadi, Electrodeposition of anionic, cationic and nonionic surfactants and gold nanoparticles onto glassy carbon electrode for catechol detection, J. Nanoanal., 6, 48 (2019).
18. Zhang R, Jin G-D, Chen D, Hu X-Y. Simultaneous electrochemical determination of dopamine, ascorbic acid and uric acid using poly(acid chrome blue K) modified glassy carbon electrode. Sensors and Actuators B: Chemical. 2009;138(1):174-81.
19. Ardakani MM, Talebi A, Naeimi H, Barzoky MN, Taghavinia N. Fabrication of modified TiO2 nanoparticle carbon paste electrode for simultaneous determination of dopamine, uric acid, and l-cysteine. Journal of Solid State Electrochemistry. 2008;13(9):1433-40.
20. Safavi A, Maleki N, Moradlou O, Tajabadi F. Simultaneous determination of dopamine, ascorbic acid, and uric acid using carbon ionic liquid electrode. Analytical Biochemistry. 2006;359(2):224-9.
21. Chauhan N, Pundir CS. An amperometric uric acid biosensor based on multiwalled carbon nanotube–gold nanoparticle composite. Analytical Biochemistry. 2011;413(2):97-103.
22 Y.T. Yin, W.D. Zhou, J. Li, and Q. Wang, A highly sensitivity and selectivity Pt-SnO_2 nanoparticles for sensing applications at extremely low level hydrogen gas detection, J. Alloys Comp., 805, 229 (2019).
23. Rajaei M, Foroughi MM, Jahani S, Shahidi Zandi M, Hassani Nadiki H. Sensitive detection of morphine in the presence of dopamine with La3+ doped fern-like CuO nanoleaves/MWCNTs modified carbon paste electrode. Journal of Molecular Liquids. 2019;284:462-72.
24. Zhu X, Yang J, Dastan D, Garmestani H, Fan R, Shi Z. Fabrication of core-shell structured Ni@BaTiO3 scaffolds for polymer composites with ultrahigh dielectric constant and low loss. Composites Part A: Applied Science and Manufacturing. 2019;125:105521.
25. Foroughi MM, Jahani S, Hassani Nadiki H. Lanthanum doped fern-like CuO nanoleaves/MWCNTs modified glassy carbon electrode for simultaneous determination of tramadol and acetaminophen. Sensors and Actuators B: Chemical. 2019;285:562-70.
26. Dastan D, Gosavi SW, Chaure NB. Studies on Electrical Properties of Hybrid Polymeric Gate Dielectrics for Field Effect Transistors. Macromolecular Symposia. 2015;347(1):81-6.
27. Safaei M, Foroughi MM, Ebrahimpoor N, Jahani S, Omidi A, Khatami M. A review on metal-organic frameworks: Synthesis and applications. TrAC Trends in Analytical Chemistry. 2019;118:401-25.
28. Dastan D, Banpurkar A. Solution processable sol–gel derived titania gate dielectric for organic field effect transistors. Journal of Materials Science: Materials in Electronics. 2016;28(4):3851-9.
29. Torkzadeh-Mahani R, Foroughi MM, Jahani S, Kazemipour M, Hassani Nadiki H. The effect of ultrasonic irradiation on the morphology of NiO/Co3O4 nanocomposite and its application to the simultaneous electrochemical determination of droxidopa and carbidopa. Ultrasonics Sonochemistry. 2019;56:183-92.
30. Yin X-T, Dastan D, Wu F-Y, Li J. Facile Synthesis of SnO2/LaFeO3–XNX Composite: Photocatalytic Activity and Gas Sensing Performance. Nanomaterials. 2019;9(8):1163.
31. Foroughi MM, Jahani S, Rajaei M. Facile Fabrication of 3D Dandelion-Like Cobalt Oxide Nanoflowers and Its Functionalization in the First Electrochemical Sensing of Oxymorphone: Evaluation of Kinetic Parameters at the Surface Electrode. Journal of The Electrochemical Society. 2019;166(14):B1300-B11.
32. Abbasi S, Hasanpour M, Ahmadpoor F, Sillanpää M, Dastan D, Achour A. Application of the statistical analysis methodology for photodegradation of methyl orange using a new nanocomposite containing modified TiO2 semiconductor with SnO2. International Journal of Environmental Analytical Chemistry. 2019:1-17.
33. Iranmanesh T, Foroughi MM, Jahani S, Shahidi Zandi M, Hassani Nadiki H. Green and facile microwave solvent-free synthesis of CeO2 nanoparticle-decorated CNTs as a quadruplet electrochemical platform for ultrasensitive and simultaneous detection of ascorbic acid, dopamine, uric acid and acetaminophen. Talanta. 2020;207:120318.
34. Hu W, Li T, Liu X, Dastan D, Ji K, Zhao P. 1550 nm pumped upconversion chromaticity modulation in Er3+ doped double perovskite LiYMgWO6 for anti-counterfeiting. Journal of Alloys and Compounds. 2020;818:152933.
35. Mirzaei H, Nasiri AA, Mohamadee R, Yaghoobi H, Khatami M, Azizi O, et al. Direct growth of ternary copper nickel cobalt oxide nanowires as binder-free electrode on carbon cloth for nonenzymatic glucose sensing. Microchemical Journal. 2018;142:343-51.
36. Dastan D, Leila Panahi S, Yengntiwar AP, Banpurkar AG. Morphological and Electrical Studies of Titania Powder and Films Grown by Aqueous Solution Method. Advanced Science Letters. 2016;22(4):950-3.
37. Khatami M, Heli H, Mohammadzadeh Jahani P, Azizi H, Lima Nobre MA. Copper/copper oxide nanoparticles synthesis using Stachys lavandulifolia and its antibacterial activity. IET Nanobiotechnology. 2017;11(6):709-13.
38. Dastan D. Effect of preparation methods on the properties of titania nanoparticles: solvothermal versus sol–gel. Applied Physics A. 2017;123(11).
39. Khatami M, Nejad MS, Almani PGN, Salari S. Plant-mediated green synthesis of silver nanoparticles using Trifolium resupinatum seed exudate and their antifungal efficacy on Neofusicoccum parvum and Rhizoctonia solani. IET Nanobiotechnology. 2016;10(4):237-43.
40. Hafaiedh I, Elleuch W, Clement P, Llobet E, Abdelghani

A. Multi-walled carbon nanotubes for volatile organic compound detection. Sensors and Actuators B: Chemical. 2013;182:344-50.
41. A. Asghar Pasban, E. Hossein Nia, and M. Piryaei, Determination of Acetaminophen Via TiO_2/MWCNT Modified Electrode, J. Nanoanal., 4, 142 (2017).
42. Aljerf L, Dastan D, Sajjadifar S, Bhatnagar S, Ukaogo PO, Dehmchi F. Guidelines for the preparation and isolation of Radionuclides produced with In-house Cyclotrons Bombardments. Open Journal of Chemistry. 2019;5(1):020-9.
43. Hernández-Gil J, Perelló L, Ortiz R, Alzuet G, González-Álvarez M, Liu-González M. Synthesis, structure and biological properties of several binary and ternary complexes of copper(II) with ciprofloxacin and 1,10 phenanthroline. Polyhedron. 2009;28(1):138-44.
44. Laviron E. General expression of the linear potential sweep voltammogram in the case of diffusionless electrochemical systems. Journal of Electroanalytical Chemistry and Interfacial Electrochemistry. 1979;101(1):19-28.
45. A.J. Bard, and L.R. Faulkner, Electrochemical Methods: Fundamentals and Applications, 2nd ed., Wiley, New York (2001).
46. Chauhan N, Pundir CS. An amperometric uric acid biosensor based on multiwalled carbon nanotube–gold nanoparticle composite. Analytical Biochemistry. 2011;413(2):97-103.
47. Prakash S, Chakrabarty T, Michael Rajesh A, Shahi VK. Investigation of polyelectrolyte for electrochemical detection of uric acid in presence of ascorbic acid. Measurement. 2012;45(3):500-6.
48. Babu RS, Prabhu P, Narayanan SS. Selective electrooxidation of uric acid in presence of ascorbic acid at a room temperature ionic liquid/nickel hexacyanoferarrate nanoparticles composite electrode. Colloids and Surfaces B: Biointerfaces. 2011;88(2):755-63.
49. Noroozifar M, Khorasani-Motlagh M, Jahromi FZ, Rostami S. Sensitive and selective determination of uric acid in real samples by modified glassy carbon electrode with holmium fluoride nanoparticles/multi-walled carbon nanotube as a new biosensor. Sensors and Actuators B: Chemical. 2013;188:65-72.